Journal of
Renewable Energy Research and Applications (RERA)
Vol. 7, No 1, 2026, 129-137 *DOI: 10.22044/rera.2026.17583.1521*

Step Configuration to Reduce Partial Shading Losses in Photovoltaic Arrays

A. Sh. Baburi, A. Mirzaei*, Y. Karimi

Yazd University, Yazd, Iran.

Received 15 March 2026; Revised Date 13 June 2026; Accepted Date 18 August 2026
**Corresponding author: mirzaei@yazd.ac.ir (A. Mirzaei)*

Abstract

Photovoltaic systems consist of multiple modules connected in series and parallel to produce a specific current and voltage. These modules may experience partial shading, leading to increased power losses, hot spots, reduced system performance, and physical damage to the modules. Various configurations are presented for connecting modules, each offering advantages in mitigating partial shading effects. This paper proposes a novel configuration called the Step configuration, inspired by the architecture of adjacent buildings sharing a common staircase. This configuration enhances the system's output power under all partial shading patterns. The method is simple, easy to implement, and cost-effective, ensuring lower power losses and higher reliability under partial shading conditions. The approach is tested on a 6×6 sample array and a 14×6 real power plant under various partial shading conditions in MATLAB/Simulink and compared with conventional configurations. According to the test results, the Step configuration produces higher output power compared to other configurations and uses less wiring than the total-cross-tied (TCT) configuration, although there is a slight difference in their output power.

Keywords: *Mismatch losses, Partial shading, Photovoltaic array configuration, Step configuration.*

1. Introduction

Countries rich in fossil fuels will soon face resource depletion. Moreover, fossil fuels cause severe air pollution and global warming, necessitating restrictions on their use for electricity generation. Additionally, nuclear energy is not a feasible option for many countries due to its risks, high installation and maintenance costs, and the advanced technology it requires. Consequently, the world is shifting toward clean and renewable energy sources that are abundantly available in nature. Solar energy is one such resource, and its demand is growing daily [1, 2].

To harness solar energy for electricity generation, solar modules and arrays are designed to convert sunlight into electrical energy. However, this conversion process faces challenges such as irradiation, temperature, and shading in solar arrays. While irradiation and temperature are natural factors that cannot be controlled, shading is an environmental factor that can be mitigated through proper array configuration to enhance performance [3, 4].

Photovoltaic (PV) systems convert photons from sunlight into electricity using the photovoltaic effect. Advances in semiconductor technology have further enhanced the potential of solar PV systems [5]. Variations in solar irradiance, shading effects, and rising cell temperatures shift the maximum power point (MPP) and reduce overall efficiency [6, 7].

Large PV arrays face challenges related to location, tilt angle, and partial shading [8, 9]. Among these, partial shading is a major concern, reducing PV array efficiency and causing mismatch losses. Solar cells and modules are connected in series and parallel to generate sufficient power for energy demands [10]. Partial shading on a module restricts the current of unshaded modules connected to it, directly reducing the output power of the PV array [11, 12]. Shading in PV modules primarily occurs due to clouds, trees, buildings, other PV modules, dust, bird droppings, etc. [13].

To address these issues, bypass diodes are traditionally used to mitigate the impact of shaded PV cells on unshaded ones. Bypass diodes provide high resistance during normal operation and low resistance under shading, preventing the isolation of shaded cells. While this technique reduces partial shading effects, its main drawback is that the current from shaded cells is not fully utilized in the output power [14, 15]. These bypass diodes are also responsible for multiple peaks in the power-voltage characteristics [16]. Among these peaks, the one with the highest power is called the global maximum power point (GMPP), while the others are local maximum power points (LMPPs). Conventional maximum power point tracking (MPPT) algorithms, such as perturb and observe (P&O) and incremental conductance, may become trapped in LMPPs. Various techniques for tracking GMPP under partial shading are presented, including artificial intelligence-based MPPT algorithms like fuzzy logic, neural networks, and hybrid methods such as simulated annealing (SA) with P&O and particle swarm optimization (PSO) with P&O [17, 18].

Different PV array configurations have been introduced to reduce mismatch losses and the number of LMPPs. Series (S), series-parallel (SP), bridge-linked (BL), and honey-comb (HC) configurations are compared under various partial shading conditions (PSC) for efficiency, power losses (PL), fill factor (FF), and GMPP. The HC configuration is found to produce the highest power in most partial shading cases [19]. An analysis of 15 configuration methods shows that the magic square (MS) method outperforms others [20]. Wiring losses in total-cross-tied (TCT), HC, and BL configurations are compared, revealing that TCT has higher wiring losses than HC and BL [21].

Other PV array configurations, such as SP, HC, BL, TCT, parallel total-cross-tied (P-TCT), bridge-linked honeycomb (BL-HC), and bridge-linked total-cross-tied (BL-TCT), are examined under shading conditions. Furthermore, the Latin square (LS) reconfiguration method is introduced, wherein the magic square total-cross-tied (MS-TCT) configuration demonstrates superior performance in terms of GMPP, power losses (PL), and fill factor (FF) [22]. The dimension-independent array reconfiguration (DIAR) and benzo (BZ) methods, applicable to symmetric and asymmetric arrays, exhibit fewer connections and lower PL than TCT, along with higher output power than HC and BL [23, 24].

The optimized Ken-Ken (KK) and Sudoku-based reconfiguration methods, employed for symmetric arrays, effectively disperse shading and reduce wiring and PL compared to TCT, BL, and HC configurations [9, 25]. Traditional configurations (S, P, SP, HC, BL, TCT) are compared with a total-tied couple linked (TTCL) method, where TTCL demonstrates better performance under shading [26]. The screw configuration, categorized into horizontal (SCR-H) and vertical (SCR-V) propagation, performs comparably but outperforms SP, Sudoku, and TCT in certain shading scenarios [27]. By employing an optimized Sudoku-based reconfiguration method for the physical arrangement of the modules in the TCT topology, the Sudoku-integrated TCT configuration achieves higher output power compared to the conventional TCT configuration alone [28]. Modeling and simulating the S, P, SP, TCT, BL, and HC configurations under different shading conditions show that the TCT configuration demonstrates the best performance [29, 30].

In this paper, a novel Step configuration is proposed and tested on a 6×6 sample array and a 14×6 real power plant under various shading conditions. Its performance is compared with conventional configurations. The rest of the paper is organized as follows: Section-II introduces various shading patterns on PV arrays and performance indices; Section-III elaborates on the proposed configuration; Section-IV provides the simulation results and comparisons of various configurations under PSC; and Section-V concludes the paper based on the simulation results.

2. Shading patterns and performance indices

To compare the configurations with each other, various shading conditions and performance indices are introduced to determine the optimal configuration.

2.1. Shading patterns

To analyze the performance of 6×6 PV sample array configurations, various shading patterns are considered, such as no shading, frame, center, L-shape (LS), short & narrow (SN), long & narrow (LN), short & wide (SW), and long & wide (LW) shading. The solar irradiance levels considered in this study are 400 W/m2, 500 W/m2, 600 W/m2, 700 W/m2, 800 W/m2, 900 W/m2 and 1000 W/m2.

When all modules receive 1000 W/m^2 of irradiance, this condition is termed no shading, as shown in figure 1(a). If the modules are shaded all around, this type of shading is called frame shading, as shown in figure 1(b). In a sample PV, the eight central modules are shaded; this type of shading is termed center shading, as shown in figure 1(c). If the first two strings and the last two rows are shaded, this type of shading is called LS shading, as shown in figure 1(d). If two strings are shaded out of six strings, and four modules are shaded per string, this type of shading is termed

SN, as shown in figure 1(e). If two strings are shaded out of six, and four modules are shaded per string, this shading type is called LN, as shown in figure 1(f). If four strings are shaded out of six, with four modules shaded per string, this shading pattern is termed SW, as shown in figure 1(g). If four strings are shaded out of six, with four modules shaded per string, this shading pattern is called LW, as shown in figure 1(h).

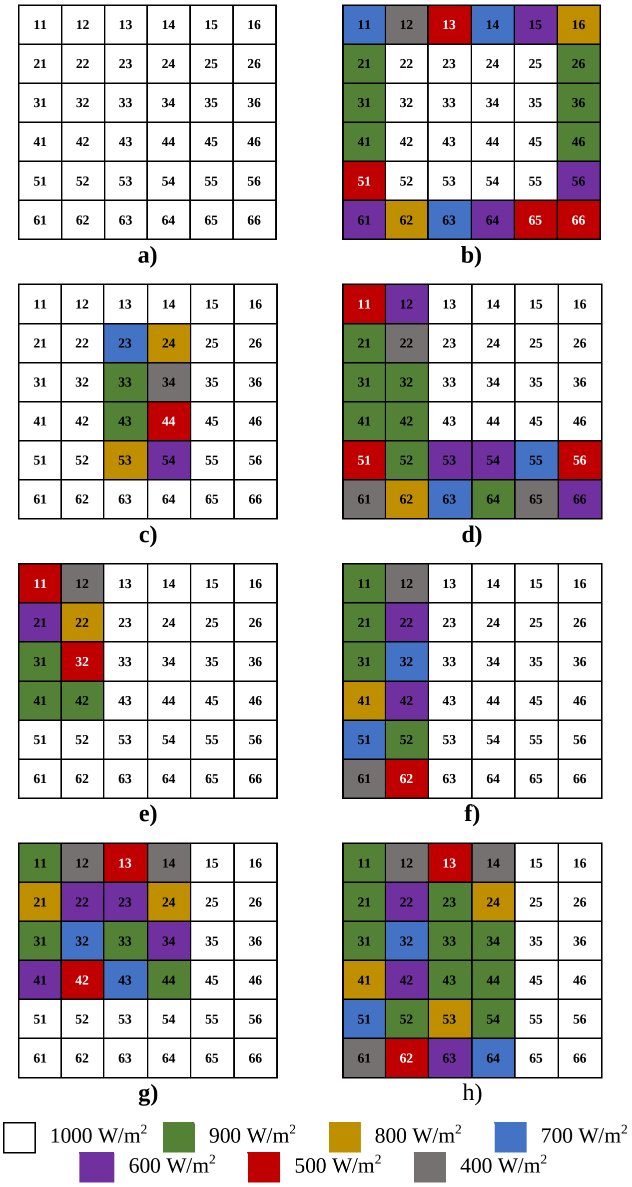

Figure 1. Various shading patterns: (a) no shading (b) frame (c) center (d) LS (e) SN (f) LN (g) SW (h) LW.

2.2. Performance indices

To evaluate the performance of configurations and compare them with each other, indicators such as performance ratio (PR), FF, mismatch losses (ML), and PL are needed to assess the performance of these configurations.

The PR is equal to the ratio of the maximum power during PSC to the maximum power under standard test conditions (STC), as shown in (1).

$$PR = \frac{P_{max} \text{ at PSC}}{P_{max} \text{ at STC}} \tag{1}$$

The FF equals the maximum power under shading divided by the product of the open-circuit voltage (V_{OC}) and the short-circuit current (I_{SC}), as shown in (2).

$$FF = \frac{P_{max} \text{ at PSC}}{V_{oc} I_{sc}} \tag{2}$$

The PL refers to the percentage of power lost by a PV array during shading. It is equal to the difference between the maximum power at STC and the maximum power under shading conditions, divided by the maximum power under STC, as shown in (3).

$$PL = \frac{P_{max} \text{ at STC} - P_{max} \text{ at PSC}}{P_{max} \text{ at STC}} \tag{3}$$

The ML refers to the power losses in the PV array during shading and is equal to the difference between the maximum power under STC and the maximum power under PSC, as shown in (4).

$$ML = P_{max} \text{ at STC} - P_{max} \text{ at PSC} \tag{4}$$

3. The proposed configuration

The proposed configuration, called the Step configuration, is inspired by a shared staircase situated between two buildings, designed for use by residents of both.

The Step configuration is proposed to mitigate partial shading effects in both symmetrical (number of modules per string equals the number of strings(and asymmetrical (number of modules per string differs from the number of strings) PV arrays. This configuration enhances the power generation of the system without requiring additional switches or sensors. The module arrangement can be determined through simple, straightforward computational steps without the need for programmable algorithms.

The mathematical procedures for calculating the Step configuration are detailed below:

- Determining the number of columns (N).
- Divide the number of columns by two, $k = \frac{N}{2}$.
- If k is an integer, connect k modules in the first row from the left, and in the second row, connect k modules from the end of the connected modules in the first row. Continue this process until reaching the end of the columns.

- When reaching the end of the columns, if the remaining modules are fewer than k, connect k modules regardless of the position of the remaining modules in the previous row.
- As with figure 2 and the previous steps, the same procedure is applied to the right side.

For an odd number of columns, follow the same steps as outlined in figure 3, with one modification: in even-numbered rows, an additional cross-connection is introduced to compensate for the odd column. This extra connection is applied on the side where shading is more likely to occur on the modules.

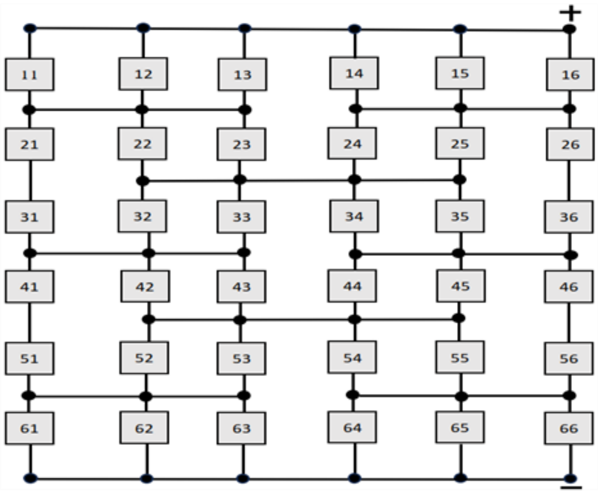

Figure 2. Step pattern for an even number of columns.

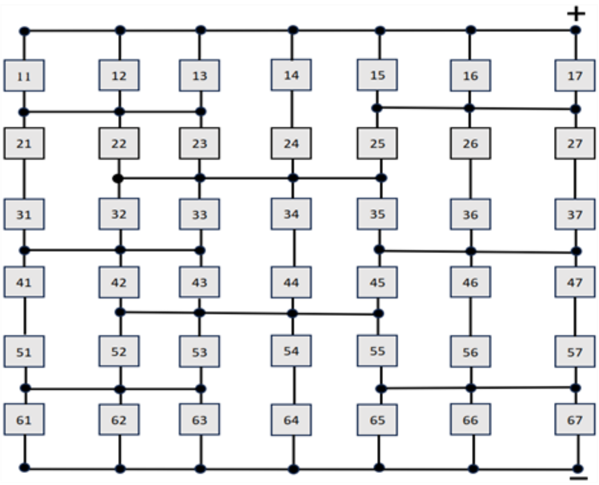

Figure 3. Step pattern for an odd number of columns.

4. Simulations and comparisons

To demonstrate the performance of the Step configuration, a 6×6 symmetric sample array and a 14×6 asymmetric real power plant are considered and compared under different shading patterns, including no shading, frame, central, LS, SN, LN, SW, and LW, using TCT, BL, HC, BZ, DIAR, and SP configurations. The results are evaluated through performance indices.

4.1. Sample array

In a 6×6 sample array, the performance of various configurations for the subsequent shading is examined.

4.1.1. No shading

In a 6×6 array without shading, all modules receive uniform irradiance of 1000 W/m², as shown in figure 1(a). Based on the simulation results, the power-voltage and current-voltage curves are illustrated in figures 4(a) and 4(b), respectively, and the performance of the sample array is presented in table 1. All configurations are similar and produce an output power of 9121 W.

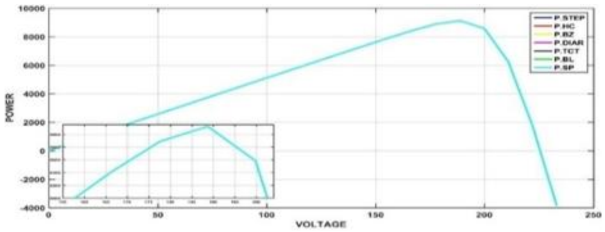

(a)

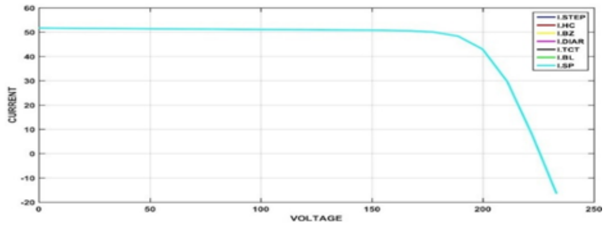

(b)

Figure 4. No shading curves (a) P-V and (b) I-V

Table 1. Sample array performance with no shading

	P (W)	PR (%)	PL (%)	ML (W)	FF (%)
Step	9121	100	0	0	79.6
HC	9121	100	0	0	79.6
BZ	9121	100	0	0	79.6
DIAR	9121	100	0	0	79.6
TCT	9121	100	0	0	79.6
BL	9121	100	0	0	79.6
SP	9121	100	0	0	79.6

4.1.2. Frame shading

In the frame shading, one module of 400 W/m^2, four modules of 500 W/m^2, four modules of 600 W/m^2, three modules of 700 W/m^2, two modules of 800 W/m^2, six modules of 900 W/m^2, and 16 modules of 1000 W/m^2 are shaded, as shown in figure 1(b). Based on the simulation results, the power-voltage and current-voltage curves are illustrated in figures 5(a) and 5(b), respectively, and the performance of the sample array is presented in Table 2. Under frame shading conditions, the TCT, Step, HC, BL, BZ, DIAR, and SP configurations produce the highest output power in that order, while the DIAR and SP exhibit similar performance.

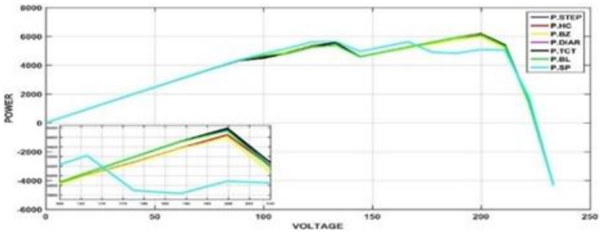

(a)

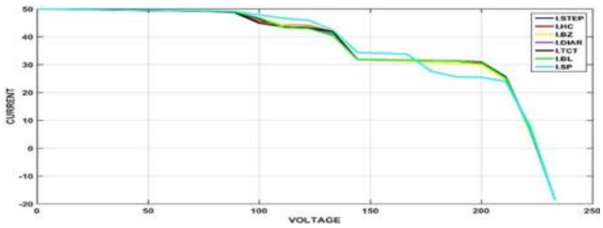

(b)

Figure 5. Frame shading curves (a) P-V and (b) I-V

Table 2. Sample array performance with frame shading

	P (W)	PR (%)	PL (%)	ML (W)	FF (%)
Step	6166	67.6	32.4	2954	53.8
HC	6050	66.3	33.7	3070	52.8
BZ	5995	65.7	34.3	3125	52.3
DIAR	5634	61.8	38.2	3486	49.2
TCT	6187	67.8	32.2	2933	54.0
BL	6133	67.2	32.8	2987	53.5
SP	5634	61.8	38.2	3486	49.2

4.1.3. Center shading

In the center shading, one module of 400 W/m^2, one module of 500 W/m^2, one module of 600 W/m^2, one module of 700 W/m^2, two modules of 800 W/m^2, two modules of 900 W/m^2, and 28 modules of 1000 W/m^2 are shaded, as shown in figure 1(c). Based on the simulation results, the power-voltage and current-voltage curves are illustrated in figures 6(a) and 6(b), respectively, and the performance of the sample array is presented in table 3. Under frame shading conditions, the TCT, Step, HC, BL, BZ, DIAR, and SP configurations produce the highest output power in that order, while the DIAR and SP exhibit similar performance.

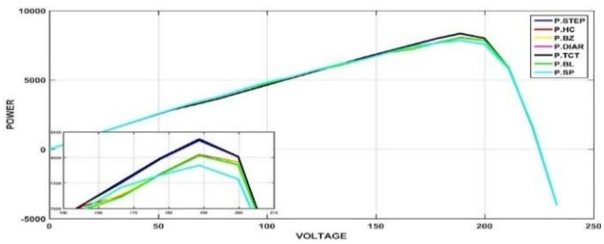

(a)

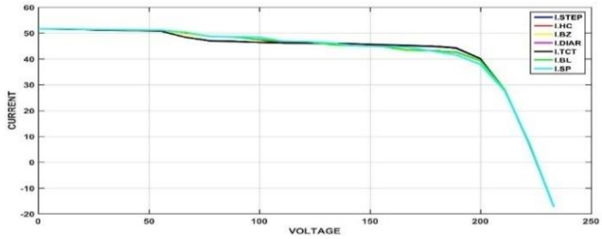

(b)

Figure 6. Center shading curves (a) P-V and (b) I-V

Table 3. Sample array performance with center shading

	P (W)	PR (%)	PL (%)	ML (W)	FF (%)
Step	8332	91.3	8.6	787	72.7
HC	8051	88.3	11.7	1069	70.3
BZ	8029	88.0	12.0	1091	70.1
DIAR	7847	86.0	14.0	1273	68.5
TCT	8362	91.7	8.3	753	73.0
BL	8037	88.1	11.9	1083	70.2
SP	7847	86.0	14.0	1273	68.5

4.1.4. LS shading

In the LS shading, three modules of 400 W/m^2, three modules of 500 W/m^2, four modules of 600 W/m^2, two modules of 700 W/m^2, one module of 800 W/m^2, seven modules of 900 W/m^2, and 16 modules of 1000 W/m^2 are shaded, as shown in figure 1(d). Based on the simulation results, the power-voltage and current-voltage curves are illustrated in figures 7(a) and 7(b), respectively, and the performance of the sample array is presented in table 4. Under LS shading conditions, the TCT, Step, HC, BZ, BL, DIAR, and SP configurations produce the highest output power in that order, while the DIAR and SP exhibit similar performance.

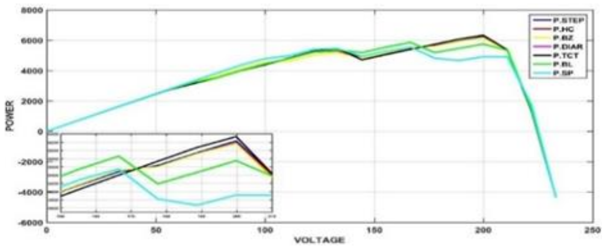

(a)

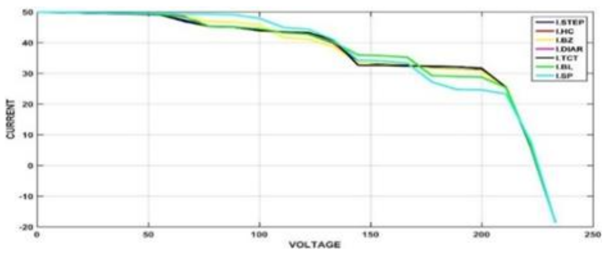

(b)

Figure 7. LS shading curves (a) P-V and (b) I-V

Table 4. Sample array performance with LS shading

	P (W)	PR (%)	PL (%)	ML (W)	FF (%)
Step	6227	68.3	31.7	2893	54.4
HC	6179	67.8	32.2	2941	53.9
BZ	6162	67.6	32.4	2958	53.8
DIAR	5549	60.8	39.2	3571	48.4
TCT	6331	69.4	30.6	2789	55.3
BL	5856	64.2	65.8	3264	51.1
SP	5549	60.8	39.2	3571	48.4

4.1.5. SN shading

In the SN shading, one module is shaded at 400 W/m^2, two modules at 500 W/m^2, one module at 600 W/m^2, one module at 800 W/m^2, three modules at 900 W/m^2, and 28 modules at 1000 W/m^2 are shaded, as shown in figure 1(e). Based on the simulation results, the power-voltage and current-voltage curves are illustrated in figures 8(a) and 8(b), respectively, and the performance of the sample array is presented in table 5. Under SN shading conditions, the TCT, Step, HC, BZ, BL, DIAR, and SP configurations produce the highest output power in that order, while the DIAR and SP exhibit similar performance.

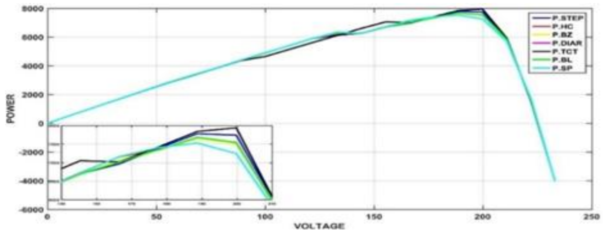

(a)

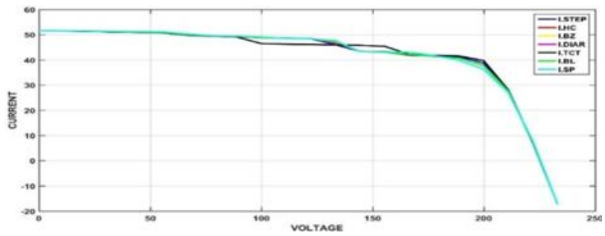

(b)

Figure 8. SN shading curves (a) P-V and (b) I-V

Table 5. Sample array performance with SN shading

	P (W)	PR (%)	PL (%)	ML (W)	FF (%)
Step	7782	8.3	14.7	1338	67.9
HC	7655	83.9	16.1	1465	66.8
BZ	7656	83.9	16.1	1464	66.8
DIAR	7529	82.5	17.5	1591	65.7
TCT	7939	87.0	13.0	1181	69.3
BL	7683	84.2	15.8	1437	67.1
SP	7529	82.5	17.5	1591	65.7

4.1.6. LN shading

In the LN shading, two modules with 400 W/m^2, one module with 500 W/m^2, two modules with 600 W/m^2, two modules with 700 W/m^2, one module with 800 W/m^2, four modules with 900 W/m^2, and 24 modules with 1000 W/m^2 are shaded, as shown in figure 1(f). Based on the simulation results, the power-voltage and current-voltage curves are illustrated in figures 9(a) and 9(b), respectively, and the performance of the sample array is presented in table 6. Under LN shading conditions, the TCT, Step, BZ, BL, HC, DIAR, and SP configurations produce the highest output power in that order, while the DIAR and SP exhibit similar performance.

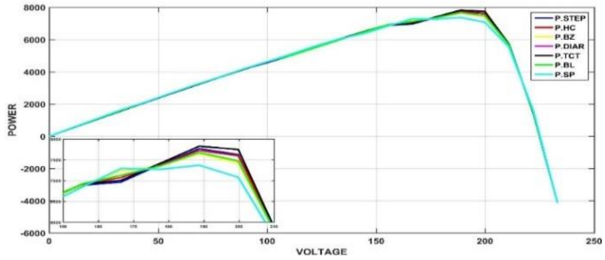

(a)

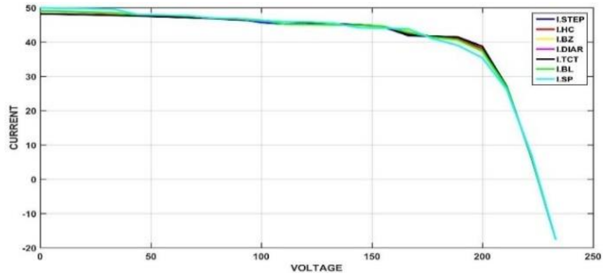

(b)

Figure 9. LN shading curves (a) P-V and (b) I-V

Table 6. Sample array performance with LN shading

	P (W)	PR (%)	PL (%)	ML (W)	FF (%)
Step	7765	85.1	14.9	1355	67.8
HC	7722	84.7	15.3	1398	67.4
BZ	7645	83.8	16.1	1475	66.7
DIAR	7367	80.8	19.2	1753	64.3
TCT	7825	85.8	14.2	1295	68.3
BL	7671	84.1	15.9	1449	67.0
SP	7367	80.8	19.2	1753	64.3

4.1.7. SW shading

In the SW shading, two modules of 400 W/m^2, two modules of 500 W/m^2, four modules of 600 W/m^2, two modules of 700 W/m^2, two modules of 800 W/m^2, four modules of 900 W/m^2, and 20 modules of 1000 W/m^2 are shaded, as shown in figure 1(g). Based on the simulation results, the power-voltage and current-voltage curves are illustrated in figures 10(a) and 10(b), respectively, and the performance of the sample array is presented in table 7. Under SW shading conditions, the TCT, Step, HC, BZ, BL, DIAR, and SP configurations produce the highest output power in that order, while the DIAR and SP exhibit similar performance.

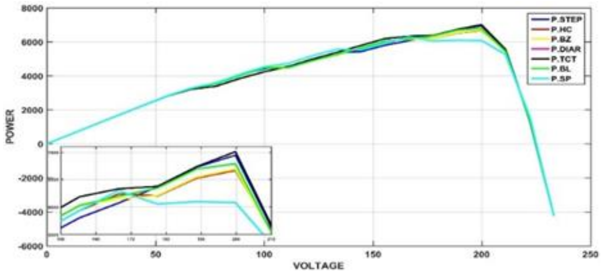

(a)

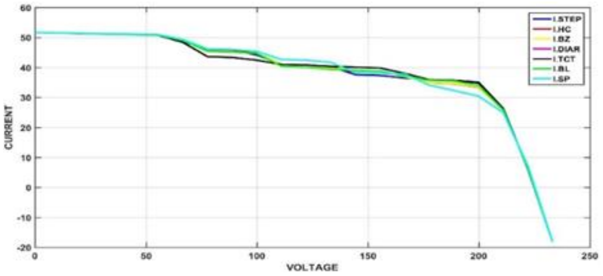

(b)

Figure 10. SW shading curves (a) P-V and (b) I-V

Table 7. Sample array performance with SW shading

	P (W)	PR (%)	PL (%)	ML (W)	FF (%)
Step	6943	76.1	23.9	2177	60.6
HC	6666	73.1	26.9	2454	58.2
BZ	6689	73.3	26.7	2431	58.4
DIAR	6298	69.1	30.9	2822	55.0
TCT	7007	76.8	23.2	2112	61.7
BL	6788	74.4	25.6	2332	59.3
SP	6298	69.1	30.9	2822	55.0

4.1.8. LW shading

In the LW shading, three modules of 400 W/m^2, two modules of 500 W/m^2, three modules of 600 W/m^2, three modules of 700 W/m^2, three modules of 800 W/m^2, ten modules of 900 W/m^2, and 12 modules of 1000 W/m^2 are shaded, as shown in figure 1(h). Based on the simulation results, the power-voltage and current-voltage curves are illustrated in figures 11(a) and 11(b), respectively, and *the* performance of the sample array is presented in table 8. Under LW shading conditions, the TCT, Step, HC, BL, BZ, DIAR, and SP configurations produce the highest output power in that order, while the DIAR and SP exhibit similar performance.

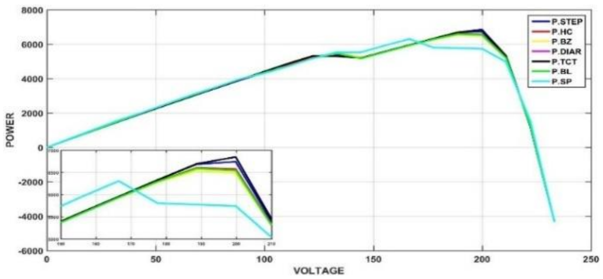

(a)

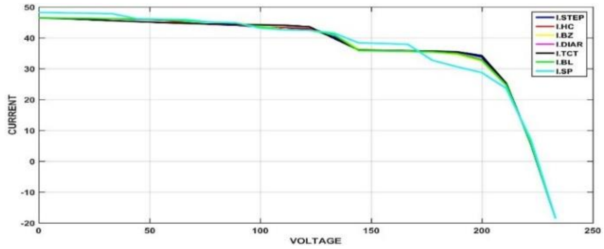

(b)

Figure 11. LW shading curves (a) P-V and (b) I-V

Table 8. Sample array performance with LW shading

	P (W)	PR (%)	PL (%)	ML (W)	FF (%)
Step	6742	73.9	26.1	2378	58.9
HC	6603	72.4	27.6	2517	57.6
BZ	6542	71.7	28.3	2578	57.1
DIAR	6305	69.1	30.9	2815	55.0
TCT	6848	75.1	24.9	2272	59.8
BL	6589	72.2	27.8	2531	57.5
SP	6305	69.1	30.9	2815	55.0

4.2. Real power plant

For better comparison of configurations, the asymmetric power plant at Yazd University is considered with dimensions of 14×6.

For this power plant, configurations with lower output power are eliminated, and only the Step, TCT, HC, and BZ configurations are retained.

The values of the performance parameters are given in Table 9. The Step configuration generates higher output power compared to other configurations and uses less wiring than the TCT configuration, although there is a slight difference in their output power. The Step configuration requires less wiring than the TCT configuration. As the size of the solar power plant increases, the amount of wiring required for the Step configuration decreases. Under partial shading conditions, a 1% reduction in power can lead to significant savings in wiring costs.

5. Conclusion

the Step configuration is inspired by the shared staircase between two buildings, designed for mutual access by residents of both structures. This novel configuration mitigates partial shading effects in PV arrays. Its performance was compared with common configurations, including HC, BZ, DIAR, TCT, BL, and SP, under diverse and complex shading conditions. This comparison was conducted on a 6×6 symmetrical sample array under seven different shading patterns: frame, central, LS, SN, LN, SW, and LW. The findings from the simulation of the sample array and the real power plant revealed that the Step configuration generates higher output power compared to other configurations and uses less wiring than the TCT configuration, although there is a slight difference in their output power.

The Step configuration is an innovative approach with significant advantages over traditional methods, as its ability to maintain optimal performance under shading conditions renders it a promising solution for maximizing output and enhancing efficiency in PV power plants. Consequently, its wider adoption is recommended, particularly in urban environments or areas prone to shading obstacles.

Table 9. Performance parameters under various partial shading condition for Step, HC, BZ and TCT

Shading Patterns	Indices	Type of Configuration			
		Step	HC	BZ	TCT
Frame	P(W)	14932	14701	14359	15188
	PR(%)	74.1	72.9	71.2	75.3
	PL(%)	25.9	27.1	28.8	24.7
	ML(W)	5229	5460	5803	4973
	FF(%)	55.9	55.0	53.7	56.8
Center	P(W)	17090	16928	16864	17135
	PR(%)	84.8	84.0	83.6	85.0
	PL(%)	15.2	16.0	16.4	15.0
	ML(W)	3072	3234	3297	3026
	FF(%)	63.9	63.3	63.1	64.1
Random	P(W)	15512	15137	15118	16510
	PR(%)	76.9	75.1	75.0	81.9
	PL(%)	23.0	24.9	25.0	18.1
	ML(W)	4650	5025	5044	3651
	FF(%)	58.0	56.6	56.6	61.8
SN	P(W)	17477	16748	16725	18159
	PR(%)	86.7	83.1	83.0	90.1
	PL(%)	13.3	16.9	17.0	9.9
	ML(W)	2685	3413	3436	2002
	FF(%)	65.4	62.7	62.6	67.9
LN	P(W)	16636	16551	16566	17591
	PR(%)	82.5	82.1	82.2	87.3
	PL(%)	17.5	17.9	17.8	12.7
	ML(W)	3525	3611	3595	2570
	FF(%)	62.2	61.9	62.0	56.2
LS	P(W)	14484	14182	13990	15017
	PR(%)	71.8	70.3	69.4	74.5
	PL(%)	28.2	29.7	30.6	25.5
	ML(W)	5678	5979	6171	5144
	FF(%)	54.2	53.1	52.3	56.2
LW	P(W)	13561	13493	13157	14620
	PR(%)	67.3	66.9	65.3	72.5
	PL(%)	32.7	33.1	34.7	27.5
	ML(W)	6601	6669	7004	5541
	FF(%)	50.7	50.5	49.2	54.7

6. References

[1] Gielena, D., Boshella, F., Saygin, D., Bazilian, M.D., Wagner, N. & Gorini, R. (2019). The role of renewable energy in the global energy transformation, Energy Strategy Reviews, vol. 24, pp. 38–50.

[2] Yousri, D., Thanikanti, S.B., Balasubramanian, K., Osama, A. & Fathy, A. (2020). Multi-objective grey wolf optimizer for optimal design of switching matrix for shaded PV array dynamic reconfiguration, IEEE Access, vol. 8, pp. 159931–159946.

[3] Sinke, W.C. (2019). Development of photovoltaic technologies for global impact, Renewable Energy, vol. 138, pp. 911–914.

[4] Satpathy, P.R., Babu, T.S., Mahmoud, A., Sharma, R. & Nastasi, B. (2021). A TCT-SC hybridized voltage equalizer for partial shading mitigation in PV arrays, IEEE Transactions on Sustainable Energy, vol. 12, no. 4, pp. 2268–2281.

[5] Parida, B., Iniyan, S. & Goic, R. (2011). A review of solar photovoltaic technologies, Renewable & Sustainable Energy Reviews, vol. 15, pp. 1625–1636.

[6] Sharma, S., Varshney, L. & Elavarasan, R.M. (2021). Performance enhancement of PV system configurations under partial shading conditions using MS method, IEEE Access, vol. 9, pp. 56630-56644.

[7] Ahmad, R., Murtaza, A.F., Sher, H.A., Shami, U.T. & Olalekan, S. (2017). An analytical approach to study partial shading effects on PV array supported by literature, Renewable & Sustainable Energy Reviews, vol. 74, pp. 721–732.

[8] Teo, J.C., Tan, R.H.G., Mok, V.H., Ramachandaramurthy, V.K. & Tan, C. (2020). Impact of bypass diode forward voltage on maximum power of a photovoltaic system under partial shading conditions, Energy, vol. 191.

[9] Pourderogar, H., Harasii, H., Alayi, R., Delbari, M. Sadeghzadeh, S.H. & Javaherbakhsh, A. (2019). Modeling and technical analysis of solar tracking system to find optimal angle for maximum power generation using MOPSO algorithm, Renewable Energy Research and Application (RERA), vol. 1, no. 2, pp. 211-222.

[10] Rajani, K. & Ramesh, T. (2021). Maximum power enhancement under partial shadings using a modified Sudoku reconfiguration, CSEE Journal of Power and Energy Systems, vol. 7, no. 6, pp. 1187-1201.

[11] Rafiqnaze, M.N. (2021). Scenario-based investigation on the effect of partial shading condition patterns for different static solar photovoltaic array configurations, IEEE Access, vol. 9, pp. 116050-116072.

[12] Srinivasan, A. (2021). L-shape propagated array configuration with dynamic reconfiguration algorithm for enhancing energy conversion rate of partial shaded photovoltaic systems, IEEE Access, vol. 9, pp. 97661-97674.

[13] Valkealahti, S. & Maki, A. (2013). Effect of photovoltaic generator components on the number of MPPs under partial shading conditions, IEEE Transactions on Energy Conversion, vol. 28, no. 4, pp. 1008-1017.

[14] D'Alessandro, V., Guerriero, P. & Daliento, S. (2014). A simple bipolar transistor-based bypass approach for photovoltaic modules, IEEE Journal of Photovoltaics., vol. 4, no. 1, pp. 505–513.

[15] Peng, B.R., Ho, K.C. & Liu, Y. H. (2018). A novel and fast MPPT method suitable for both fast changing and partially shaded conditions, IEEE Transactions on Industrial Electronics, vol. 65, no. 4, pp. 3240–3251.

[16] Alajmi, B.N., Ahmed, K.H., Finney, S.J. & Williams, B.W. (2013). A maximum power point tracking technique for partially shaded photovoltaic systems in microgrids, IEEE Transactions on Industrial Electronics, vol. 60, no. 4, pp. 1596–1606.

[17] Pankaj, V., Bharat, G., Gaurav, J. & Ravi, H. (2024). A new global maximum power point algorithm for dynamic shading patterns of partial shading, Renewable Energy Research and Application (RERA), vol. 5, no. 2, pp. 211-220.

[18] Mohapatra, M.A., Mohapatra, A., Nayak, B., Das, P. & Mohanty, K.B. (2017). A review on MPPT techniques of PV system under partial shading condition, Renewable & Sustainable Energy Reviews, vol. 80, pp. 854–867.

[19] Mikkili, S. (2018). Modeling, simulation, and performance analysis of PV array configurations (series, series-parallel, bridge linked, and honey-comb) to harvest maximum power under various partial shading conditions, International Journal of Green Energy, vol. 15, no. 13, pp. 795–812.

[20] Devakirubakaran, S., Verma, R., Chokkalingam, B. & Mihet-Popa, L. (2023). Performance evaluation of static PV array configurations for mitigating mismatch losses, IEEE Access, vol. 11, pp. 47725-47749.

[21] Rajani, K. & Ramesh, T. (2022). Reconfiguration of PV arrays (T-C-T, B-L, H-C) considering wiring resistance, CSEE Journal of Power and Energy Systems, vol. 8, no. 5, pp. 1408–1416.

[22] Pachauri, R.K., Kansal, I., Babu, T.S. & Alhelou, H.H. (2021). Power losses reduction of solar PV systems under partial shading conditions using re-allocation of PV module-fixed electrical connections, IEEE Access, vol. 9, pp. 94789-94812.

[23] Mallick, P., Sharma, R., Satpathy, P.R., Thanikanti, S.B. & Nwulu, N.I. (2023). A dimension-independent array relocation (DIAR) approach for partial shading losses minimization in asymmetrical photovoltaic arrays, IEEE Access, vol. 11, pp. 63176-63196.

[24] Saiprakash, C., Mohapatra, A., Nayak, B., Babu, T.S. & Alhelou, H.H. (2022). A novel benzene structured array configuration for harnessing maximum power from PV array under partial shading condition with reduced number of cross ties, IEEE Access, vol. 10, pp. 129712-129726.

[25] Palpandian, M., Winston, D.P., Kumar, B.P., Kumar, C.S., Babu, T.S. & Alhelou, H.H. (2021). A new ken-ken puzzle pattern based reconfiguration technique for maximum power extraction in partial shaded solar PV array, IEEE Access, vol. 9, pp. 65824-65837.

[26] Ramesh, T., Rajani, K. & Panda, A.K. (2021). A novel triple-tied-cross-linked PV array configuration with reduced number of cross-ties to extract maximum power under partial shading conditions, CSEE Journal of Power and Energy Systems, vol. 7, no. 3, pp. 567-581.

[27] Kumar, B.P. (2022). Performance enhancement of partial shaded photovoltaic system with the novel screw pattern array configuration scheme, IEEE Access, vol. 10, pp. 1731-1744.

[28] Horoufiany, M. & Ghandehari, R. (2018). Optimization of the Sudoku based reconfiguration technique for PV arrays power enhancement under mutual shading conditions, Solar Energy, vol. 159, pp. 1037-1046.

[29] Bingol, O. & Ozkaya, B. (2018). Analysis and comparison of different PV array configurations under partial shading conditions, Solar Energy, vol. 160, pp. 336-343.

[30] Niti, A. (2025) Performance of partially shaded series-parallel and total-cross-tied configured PV array, Renewable Energy Research and Applications (RERA), vol. 6, no. 1, pp. 61-73.